# Ligand Conjugation Directs Formation of a 1,3-Dihydropyridinate Regioisomer

Tobias J. Sherbow, Leo W. T. Parsons, Nathan A. Phan, James C. Fettinger and Louise A. Berben*

Department of Chemistry, University of California One Shields Ave, Davis, CA 95616 (USA)

**ABSTRACT:** The selective formation of the 1,4-dihydropyridine isomer of NAD(P)H is mirrored by the selective formation of 1,4-dihydropyridinate ligand-metal complexes in synthetic systems. Here we demonstrate that ligand conjugation can be used to promote selective 1,3-dihydropyridinate formation. This represents an advance toward controlling and tuning selectivity in dihydropyridinate formation chemistry. Reaction of ($I_2P^{2-}$)Al(THF)Cl (**1**) ($I_2P$ = bis(imino)pyridine) with the one-electron oxidant, TEMPO, afforded ($I_2P^{-}$)AlCl(TEMPO) (**2**) which can be reduced with Na to the twice-reduced ligand complex ($I_2P^{2-}$)Al(TEMPO) (**3**). Compounds **2** and **3** serve as precursors for high yielding and selective routes to an Al-supported 1,3-dihydropyridinate complex via reaction of **2** with three equivalents of K metal, or reaction of **3** with KH.

## INTRODUCTION

In biological systems, organic cofactors such as pyridine nucleotide, NAD(P)H, execute electron transfer (ET), proton transfer (PT) and hydride transfer reaction chemistry with exquisite regioselectivity. The catalytic reactions performed by NAD(P)H are selective in the formation of the organohydride (Scheme 1, top): 1,4-dihydropyridine (1,4-DHP), and they are chemoselective in the step where a hydride is transferred to the substrate. The role of the protein environment surrounding DHP's, the mechanism of DHP reaction chemistry,[1] and the role of the DHP side-chains,[2] have been probed and model systems for these efforts including dihydrofolate reductase (DHFR),[3] and aldehyde dehydrogenases,[4] have been studied in detail. Along with these ongoing efforts in biological systems, there is significant scope to enhance our understanding of organohydride chemistry via synthetic approaches. [5,6,7,8]

In synthetic systems, selectivity for a particular isomer of DHP is difficult to realize (Scheme 1, bottom). Another of the many differences between biological and synthetic DHP's is that the synthetic chemistry occurs at very high reduction potentials, typically more negative than -2.0 V vs. SCE. Use of an NADH model as an electrochemical mediator has been achieved,[9] and examples where NADH regeneration is catalyzed by a co-enzyme illustrate the ability of the biological system to lower the overpotential for that process.[10,11] Elegant work using NADH-inspired organohydrides as hydride transfer reagents also illustrates that electrochemical turnover to regenerate the organohydride requires a high overpotential,[12,13] and these findings were corroborated by thermochemical analyses.[14,15] One approach to lowering the energy of synthetic DHP chemistry is to associate a $DHP^-$ molecule as a ligand to a redox inactive Lewis acidic metal center such as Mg(II), Zn(II), or Al(III). These ions can lower the redox potential for ET via electrostatic and inductive effects. Similarly, Mg(II),[16] Zn(II),[17] and Mn(II)[18] ions interact with NAD(P)H in biological systems although the precise role(s) of those metals in the biological systems is not yet fully understood.

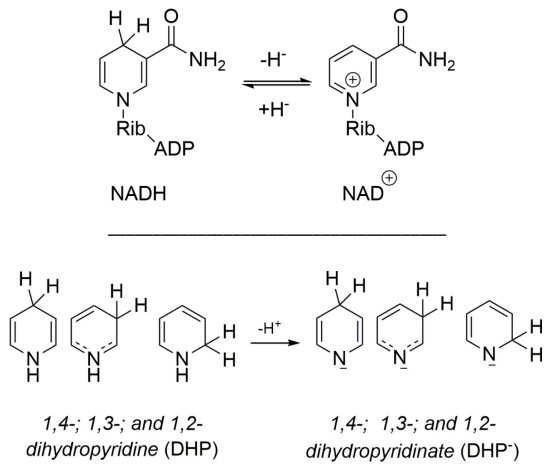


**Scheme 1. (top) Schematic of nicotinamide adenine dinucleotide (NADH): Rib = ribose ring, ADP = adenine diphosphate. (bottom) Dihydropyridine (DHP), and dihydropyridinate ($DHP^-$) isomers.**

Examples of selective 1,4-$DHP^-$ formation in synthetic systems include many instances where the *N*-atom of 1,4-$DHP^-$ (or pyridine) is one of the donor atoms centered in a symmetric tridentate ligand such as a bis(imino)pyridine (Scheme 2). These examples include 1,4-$DHP^-$ formation with redox-active metal coordination complexes such as Ni or Mo,[19,20] and cases where 1,4-$DHP^-$ is stabilized by coordination to Lewis acidic metals such as U(III) or Al(III).[21,22] Presumably, the mirror symmetry of the tridentate ligands contributes to the observed selectivity for the 1,4-$DHP^-$ regioisomer in all of these known examples. Specific to the bis(imino)pyridine ligand system ($I_2P$), one example of 1,4-$DHP^-$ formation has been reported in 10% yield, by the reaction of $I_2P$ with Al($^i$Bu)$_2$H.[23]

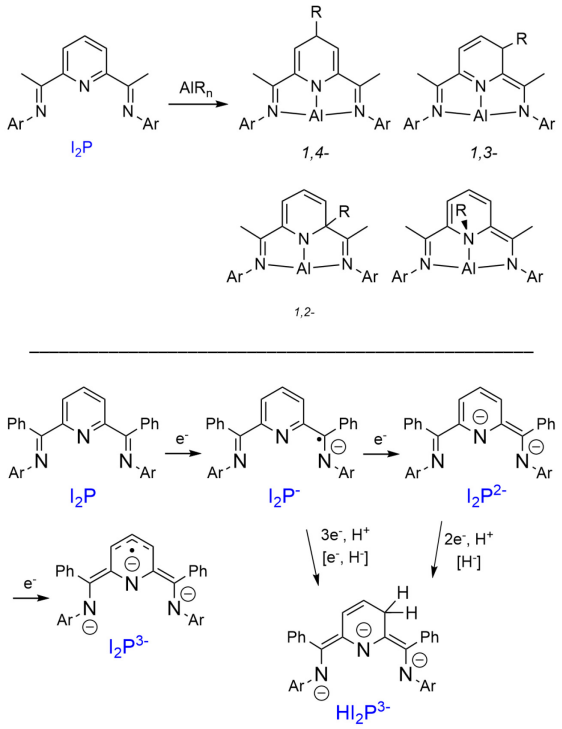

**Scheme 2. (top) Bis(imino)pyridine, left. Possible isomers of alkylated bis(imino)pyridinate, right. (bottom) $I_2P$ in various charge states. Only the form with a 3- charge limits $DHP^-$ regioselectivity to one isomer. Ar = diisopropylphenyl. See SI for possible regioisomers of $I_2P$, $I_2P^-$, and $I_2P^{2-}$ charge states.**

In other work with $I_2P$, control of regioselectivity has been targeted by alkylation of pyridyl rings so that the alkyl substituent directs the regioselectivity of subsequent hydride formation (Scheme 2). However, the alkylation is not regioselective except in a handful of cases. In those examples, the regioselectivity of alkylation is unpredictable even if it is selective.[24,25,26,27] Regarding the alkylation of $I_2P$ ligands coordinated to Al(III), mixtures of products are obtained with 1,4-, 1,3- and 1,2- substitution patterns.[28] In all of those prior examples, the metal-supported alkyl-substituted R-$I_2P$ ligand is formed by addition of $R^-$ to the uncharged $I_2P$ which provides no energetic preference for one isomer over another. If alkyl or hydride were added to the $I_2P$ or $I_2P^-$ charge states those reactions would also be expected to afford multiple isomers of $HI_2P^-$ or $HI_2P^{2-}$, respectively (Scheme S1).

In the foregoing report, we explore the protonated 3- charge state of the $I_2P$ ligand (denoted as $HI_2P^{3-}$) because it will likely be able to support formation of the 1,3-$DHP^-$ regioisomer of $DHP^-$. 1,3-$DHP^-$ should form selectively due to the influence of the ligand conjugation since the 2- and 6-carbons of the $DHP^-$ ring form C-C double bonds with the imino carbon atoms (Scheme 2 bottom). Similarly, formation of the 1,4-DHP isomer of NADPH is directed by ligand structure where the pyridyl ring π-system is in conjugation with the amide side-chain (Scheme 1).[2] Prior studies have demonstrated that side-chain substitutions such as an aldehyde that preserves the conjugation retain activity in LDH, whereas side-chain substitutions including no conjugation result in loss of functionality. Access to the 3- charge state of $I_2P$ is itself thermodynamically challenging, but was achieved by complexation of Lewis acidic Al(III) to the $I_2P$ ligand. The open coordination site on Al(III) was protected by a TEMPO ligand (TEMPO = (2,2,6,6-Tetramethylpiperidin-1-yl)oxyl) which is stable under the redox conditions employed in formation of the $DHP^-$-containing $HI_2P^{3-}$ ligand. The reaction in which TEMPO is installed onto the Al center represents a first example of ligand substitution at Al that is facilitated by $I_2P$ ligand redox cycling.

## RESULTS AND DISCUSSION

The starting reagent for this work is ($I_2P^{2-}$)Al(THF)Cl (**1**) which was previously reported.[29] Our initial attempts to access reduced $DHP^-$ complexes of Al(III) explored the reduction of $I_2P$-supported Al(III) complexes such as **1** and ($I_2P^-$)$AlCl_2$ with various equivalents of Na metal- or K metal-based reductants. These reactions afforded dark intractable solutions from which no products could be identified despite numerous efforts. Further attempts to access DHP chemistry supported by Al(III) employed the reaction of **1** with hydride transfer reagents, but these also afforded unfavorable mixtures of products corroborating those reported by past work with the analogous alkyl transfer reactions (*vide supra*). In combination, these efforts ultimately led to the realization that, in many cases, elimination of NaCl or KCl promoted by the in situ generation of $Na^+$ or $K^+$ cations in those reduction and hydride transfer reactions may leave the Al center unprotected. We turned instead to replacing the chloro ligand in **1** with *O*-donor ligands which might exploit the known oxophilicity of Al(III) to afford a metal-ligand interaction that is stable under the redox conditions needed to generate reduced $DHP^-$'s (Scheme 3).

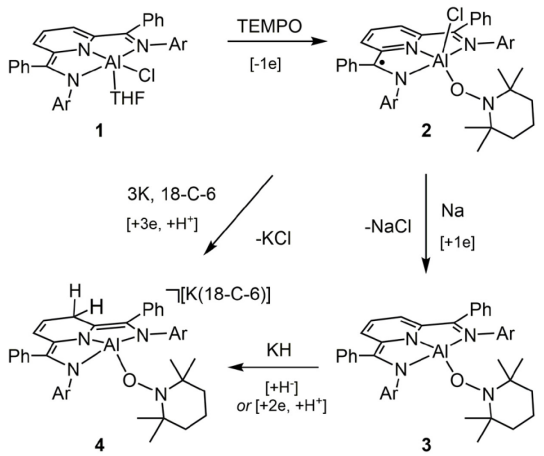

**Scheme 3. Synthesis of complexes 2 – 4 from 1. Ar = diisopropylphenyl.**

Accordingly, reaction of **1** with 1 equiv TEMPO in benzene at room temperature resulted in an immediate color change from orange-brown to deep red and produced the one-electron oxidized Al-nitroxido complex ($I_2P^-$)Al(TEMPO)Cl (**2**) in a near quantitative yield of 95% (Scheme 3). Single crystal X-ray diffraction data and magnetic susceptibility of $\mu_{eff}$ = 1.63 $\mu_B$ support the assignment that a ligand-based one-electron oxidation $I_2P^-$ product is formed from the $I_2P^{2-}$ reactant. Red crystals of **2** were grown as plates from concentrated hexane solutions held at -25 °C, and the coordination

geometry around Al(III) is best described as a distorted trigonal bipyramid (Figure 1, Tables S1 and S2). The five-coordinate complex has one mono-anionic tridentate $I_2P^-$ ligand, one chloro, and one nitroxide TEMPO ligand. In free TEMPO, the N-O bond length is 1.283(9) Å.[30] There are two unique molecules of **2** in the unit cell and the average of the two N-O bond lengths are 1.445(3) Å, confirming that a one-electron reduction of TEMPO occurred as seen in prior examples of TEMPO reduction. Additionally, the averaged Al—O bond lengths of 1.768(2) Å and are consistent with an Al—O oxide bond length.[31] This consistency further confirms that the one-electron reduction of TEMPO was effected. The bond lengths of the $I_2P$ ligand are consistent with a 1- charge on the tridentate ligand, where the two $N_{im}$—$C_{im}$ bond lengths are 1.320(3) Å and 1.337(3) Å in **2**, and localization of the single added electron is on the C atom of one imino donor.[32]

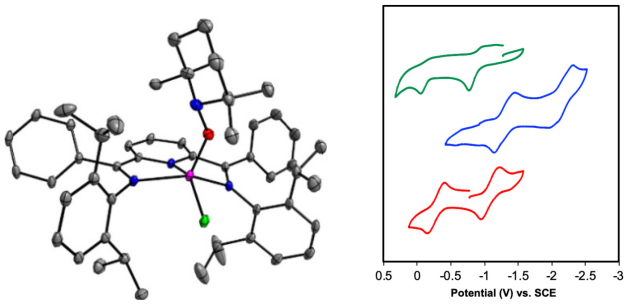


**Figure 1.** (left) Solid-state structure of ($I_2P^-$)Al(TEMPO)Cl in **2**. Pink, red, blue, green and grey ellipsoids represent Al, O, N, Cl and C atoms, respectively. Ellipsoids are shown at 30% probability level. Solvent and H atoms omitted for clarity. (right) CV of 1mM **2** collected in 0.3 M $NBu_4PF_6$ THF solution. 100 mV/s, GC electrode. CV's of 1 mM solutions of **2** (red), **3** (blue) and **4** (green) collected in 0.3 M $NBu_4PF_6$ THF solution. 100 mV/s, GC electrode.

In the CV of **2,** a reversible redox event is observed at -1.13 V vs. SCE, which suggested to us that **2** can be further reduced and that the N-O bond should remain intact allowing the reduction of the $I_2P$ ligand (Figure 1 right). There was no evidence for chloro dissociation in the CV's collected between 50 – 500 mV/s, and the peak-to-peak separation ($E_p$ = 210 mV) is consistent with reversible data, when CV's are collected in THF. It is known that the N-O bond in TEMPO is sometimes susceptible to reduction to promote N-O bond cleavage, but in other instances the N-O bond can be quite resistant to a wide array of reaction conditions.[33] Cleavage of the N-O bond most often occurs when intermediates can be stabilized by an M-oxo multiple bond character, as in the one-electron reduction of a phenyltris(imidazolyl)borate Fe(II) TEMPO complex to give a transient Fe=O that performs *O*-atom transfer reactions.[34]

A deep red solution of **2** was stirred with one equivalent of Na in benzene for 24 hours and this afforded a dark yellow-brown colored solution. Proton NMR spectroscopic analysis of the resulting diamagnetic compound, along with single crystal X-ray analysis, identified ($I_2P^{2-}$)Al(TEMPO) (**3**) and NaCl as the byproduct from this reaction (Scheme 2, Figure S1). The triplet proton NMR resonance associated with the *para*-pyridine H-atom was observed at 5.79 ppm which is upfield of the resonance at 5.93 ppm for ($I_2P^{2-}$)AlCl.[35] This result is consistent with the more donating TEMPO ligand in comparison with chloro. Single crystals of **3** were grown as brown blocks from a concentrated hexane solution held at -25 °C. (Figure 2, Tables S1 and S2). The $I_2P^{2-}$ ligand in **3** is asymmetric with alternating single and double C-C bonds which can be described as the $N_{im}$—$C_{im}$ and $N_{am}$—$C_{am}$ bond lengths which are 1.3465(18) Å and 1.4143(18) Å, respectively. In **3** the Al—O bond length decreases to 1.7181(11) Å from 1.771(2) Å in **2**, and this shortening is attributed to the loss of the chloro ligand that potentially increased the ionic interaction between Al and TEMPO. The $N_{py}$-Al-O bond angles are 101.24(10) and 128.36(5) Å for **2** and **3**, respectively. The large size of TEMPO prevents formation of the SP geometry for **3**. The four-coordinate geometry index for **3** is $\tau_4$ = 0.69 and indicates that it is closer to a tetrahedral geometry.[36]

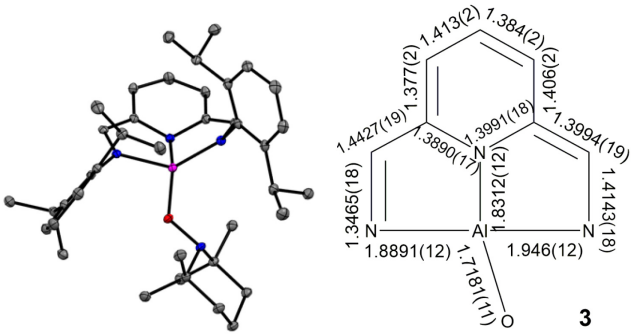


**Figure 2.** (left) Solid-state structure of [($^{Ph}I_2P^{2-}$)Al(TEMPO)] in **3**. (right) Line drawing of **3**. Pink, red, blue, and grey ellipsoids represent Al, O, N, and C atoms, respectively. Ellipsoids shown at 30% probability. H atoms omitted for clarity.

In the CV of complex **3**, two reversible redox events are observed at -1.295 and -2.165 V vs. SCE (Figure 1), which suggested to us that **3** can be further reduced by up to two-reducing equivalents. The reversibility in the CV suggested that the N-O bond remained. The foregoing results show that when the Al center is protected by the TEMPO ligand it becomes possible to reduce $I_2P^-$ in **2** to $I_2P^{2-}$ in **3** without any significant side reactions such as N-O bond cleavage. The isolated yield of **3** was 68% which suggests a relatively clean reaction. To further explore the reduction of the $I_2P$ ligands and the formation of DHP-'s supported by Al(III) we added three equivalents of K metal to a solution of **2** in the presence of 18-crown-6 (or 18-C-6). Following crystallization from THF/hexanes [($HI_2P^{3-}$)Al(TEMPO)][K(18-C-6)(THF)$_2$] (**4**) was isolated in 82% yield (Scheme 3). The charge and protonation state of the ligands in **4** were assigned using data acquired by single crystal X-Ray diffraction and proton NMR spectroscopy and is consistent with the combustion analysis and $^{13}C$ NMR spectral data. The open circuit potential of **4** at -1.275 V vs. SCE is, as expected, more negative than that of **2** and **3** at -0.766 and -0.912 V vs. SCE, respectively (Figure 1). The CV of **4** displays two irreversible oxidation events at -0.784 and -0.060 V vs. SCE. Scanning in the negative direction did not show any additional redox events within the solvent window.

The solid-state structure of **4**, the proton NMR spectrum, and the high yielding synthesis reveal a highly selective formation of Al-supported 1,3-DHP-. The 1,3- substitution

pattern is consistent with the $^1$H NMR spectrum which shows an asymmetric molecule where four DHP$^-$ proton resonances occur at 6.36, 6.06, 3.38 and 2.77 ppm (Figure S2). Single crystals of **4** were grown from a concentrated THF solution with hexanes layered on top and then stored at -25 °C overnight (Figure 3). The four-coordinate Al center is flanked by three amido *N* donor atoms from the $HI_2P^{3-}$ ligand and one nitroxide ligand so that the complex is formally an aluminate that is charge balanced by [K(18-C-6)(THF)$_2$]. There are two independent molecules of **4** within the unit cell and we report the averages of these distances. The $C_o$-$C_m$ and $C_m$-$C_p$ distances of 1.507(3) Å and 1.514(3) Å, respectively are the two longest bonds in the DHP$^-$ ring and they flank the *meta*-carbon which is $sp^3$ hybridized as is seen by the $C_o$-$C_m$-$C_p$ bond angle of 108.44(19)°.

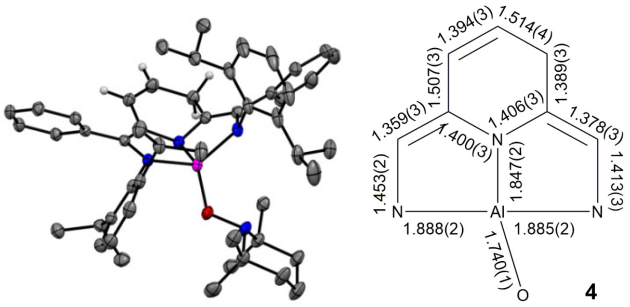


**Figure 3.** (left) Solid-state structure of [($HI_2P^{3-}$)Al(TEMPO)]$^-$ in **4**. (right) Line drawing of **4**. Pink, red, blue, and grey ellipsoids represent Al, O, N, and C atoms, respectively. Ellipsoids shown at 30% probability. [K(18-C-6)(THF)$_2$]$^+$, solvent, and H atoms except the C-H's of pyridine in **4** have been omitted for clarity.

Formation of **4** is formally a three-electron reduction and single protonation of **2** which suggests that all three equivalents of K metal are consumed in the reaction while a proton is scavenged, presumably from trace water in the THF solvent or by C-H bond activation of the isopropyl substituents on the $I_2P$ ligand. When the reaction was performed in $d_8$-THF, the same product was obtained with no proton NMR spectroscopic evidence of deuterium incorporation. In a sperate reaction a solution of **3** was stirred with one equivalent of KH and 18-C-6. Upon workup, **4** was isolated and characterized by proton NMR spectroscopy and single-crystal X-ray crystallography (Scheme 3). From this reaction, the yield of **4** was modest at 18 %, but no other products containing $I_2P$ coordinated to Al(III) could be detected. This alternative route to formation of the 1,3-DHP$^-$ isomer of **4** further highlights the selectivity for formation of 1,3-DHP$^-$ when it is supported by the [($HI_2P^{3-}$)Al(TEMPO)]$^-$ scaffold.

## CONCLUSION

In conclusion, we have demonstrated that $I_2P$ complexes of Al(III) can be protected at the Al center by the TEMPO ligand. In addition, formation of the TEMPO complex is achieved via redox cycling on the ligand that accompanies Al-O bond formation, and this represents a first example os ligand substitution at the Al center that is enabled by redox cycling on the I2P ligand. In subsequent reactions, the TEMPO ligand prevents Al-based reaction chemistry and enables redox cycling and proton transfer chemistry that takes place solely on the redox-active $I_2P$ ligand and spans ligand charge states between 1- and protonated 3-. Access to the $HI_2P^{3-}$ charge state is particularly important because that ligand conjugation pattern selectively directs formation of a single isomer of the DHP$^-$ ligands; 1,3-dihydropyridinate. Regioselective access to the 1,3-DHP$^-$ was achieved via a three-electron reduction of **2**, containing $I_2P^-$. This same 1,3- DHP$^-$ ligand was accessed via a hydride transfer reaction to **3** which contains the $I_2P^{2-}$ ligand.

These results advance previously known biological and synthetic DHP chemistry which uniquely proceeds through the 1,4-DHP isomer. The future continuation of this work can include further investigations that build on the selective DHP$^-$ chemistry of Al(III) coordination complexes including a deeper understanding of their thermochemical properties and control of selectivity in reaction chemistry. Ultimately, control of regioselectivity in DHP$^-$ formation and reactivity using the influence of Lewis acidic cations to lower the energy of reaction pathways, could expand the scope of accessible hydride transfer reaction chemistry.

## ASSOCIATED CONTENT

### Supporting Information

Crystallographic Information (CIF)

Experimental methods, crystallographic information, NMR spectra, electrochemical data (PDF)

This material is available free of charge via the Internet at http://pubs.acs.org.

## AUTHOR INFORMATION

### Corresponding Author

*laberben@ucdavis.edu

### Author Contributions

All authors have given approval to the final version of the manuscript.

## ACKNOWLEDGMENT

This manuscript was based on work supported by the National Science Foundation with award CHE-1763821. This work is dedicated to Prof. Marylin M. Olmstead, a dedicated mentor who will be dearly missed.

## REFERENCES

[1] Zheng, J.; Chen, Y. Q.; Callender, R. A study of the binding of NADP coenzymes to dihydrofolate reductase by raman difference spectroscopy. *Eur. J. Biochem.* **1993**, *215*, 9-16.

[2] Anderson, V. E.; LaReau, R. D. Hydride transfer catalyzed by lactate dehydrogenase displays absolute stereospecificity at C4 of the nicotinamide ring. *J. Am. Chem. Soc.* **1988**, *110*, 3695-3697.

[3] Liu, C. T.; Francis, K.; Layfield, J. P.; Huang, X.; Hammes-Schiffer, S.; Kohen, A.; Benkovic, S. J. *Escherichia coli* dihydrofolate reductase catalyzed proton and hydride transfers: Temporal order and the roles of Asp27 and Tyr100. *Proc. Natl. Acad. Sci. U.S.A* **2014**, *111*, 18231-18236.

[4] Konno, H.; Sakamoto, K.; Ishitani, O. Regiospecific Hydride Transfer from cis-[Ru(bpy)2(CO)(CHO)]+ to NAD+ Model Compounds: A Model for Enzymatic Reactions by Aldehyde Dehydrogenases. *Angew. Chem. Int. Ed.* **2000**, *39*, 4061-4063.

[5] Han Lee, I.-S.; Jeoung, E. H.; Kreevoy, M. M. Primary Kinetic Isotope Effects on Hydride Transfer from 1,3-Dimethyl-2-phenylbenzimidazoline to NAD+ Analogues. *J. Am. Chem. Soc.* **2001**, *123*, 7492-7496.

[6] Koga, K.; Matsubara, Y.; Kosaka, T.; Koike, K.; Morimoto, T.; Ishitani, O. Hydride Reduction of NAD(P)+ Model Compounds with a Ru(II)–Hydrido Complex. *Organometallics* **2015**, *34*, 5530-5539.

[7] Lansbury, P. T.; Peterson, J. O. Lithium Tetrakis-(N-dihydropyridyl)-aluminate: Structure and Reducing Properties. *J. Am. Chem. Soc.* **1963**, *85*, 2236-2242.

[8] McSkimming, A.; Colbran, S. B. The coordination chemistry of organo-hydride donors: new prospects for efficient multi-electron reduction. *Chem. Soc. Rev.* **2013**, *42*, 5439-5488.

[9] Smith, P. T.; Weng, S.; Chang, C. J. An NADH-Inspired Redox Mediator Strategy to Promote Second-Sphere Electron and Proton Transfer for Cooperative Electrochemical CO2 Reduction Catalyzed by Iron Porphyrin. *Inorg. Chem.* **2020**, *59*, 9270-9278.

[10] Yuan, M.; Kummer, M. J.; Milton, R. D.; Quah, T.; Minteer, S. D. Efficient NADH Regeneration by a Redox Polymer-Immobilized Enzymatic System. *ACS Catal.* **2019**, *9*, 5486-5495.

[11] Cracknell, J. A.; Vincent, K. A.; Armstrong, F. A. Enzymes as Working or Inspirational Electrocatalysts for Fuel Cells and Electrolysis. *Chem. Rev.* **2008**, *108*, 2439-2461.

[12] Ilic, S.; Pandey Kadel, U.; Basdogan, Y.; Keith, J. A.; Glusac, K. D. Thermodynamic Hydricities of Biomimetic Organic Hydride Donors. *J. Am. Chem. Soc.* **2018**, *140*, 4569-4579.

[13] Ilic, S.; Alherz, A.; Musgrave, C. B.; Glusac, K. D. Importance of proton-coupled electron transfer in cathodic regeneration of organic hydrides. *Chem. Commun.* **2019**, *55*, 5583-5586.

[14] Ilic, S.; Alherz, A.; Musgrave, C. B.; Glusac, K. D. Thermodynamic and kinetic hydricities of metal-free hydrides. *Chem. Soc. Rev.* **2018**, *47*, 2809-2836.

[15] Wiedner, E. S.; Chambers, M. B.; Pitman, C. L.; Bullock, R. M.; Miller, A. J. M.; Appel, A. M. Thermodynamic Hydricity of Transition Metal Hydrides. *Chem. Rev.* **2016**, *116*, 8655-8692.

[16] Quitterer, F.; Beck, P.; Bacher, A.; Groll, M. Structure and Reaction Mechanism of Pyrrolysine Synthase (PylD). *Angew. Chem. Int. Ed.* **2013**, *52*, 7033-7037.

[17] Dołęga, A. Alcohol dehydrogenase and its simple inorganic models. *Coord. Chem. Rev.* **2010**, *254*, 916-937.

[18] Jin, X.; Foley, K. M.; Geiger, J. H. The Structure of the 1l-myo-inositol-1-phosphate Synthase-NAD+-2-deoxy-d-glucitol 6-(E)-Vinylhomophosphonate Complex Demands a Revision of the Enzyme Mechanism. *J. Biol. Chem.* **2004**, *279*, 13889-13895.

[19] Lapointe, S.; Khaskin, E.; Fayzullin, R. R.; Khusnutdinova, J. R. Nickel(II) Complexes with Electron-Rich, Sterically Hindered PNP Pincer Ligands Enable Uncommon Modes of Ligand Dearomatization. *Organometallics* **2019**, *38*, 4433-4447.

[20] Kundu, S.; Brennessel, W. W.; Jones, W. D. Synthesis and Reactivity of New Ni, Pd, and Pt 2,6-Bis(di-tert-butylphosphinito)pyridine Pincer Complexes. *Inorg. Chem.* **2011**, *50*, 9443-9453.

[21] Mehdoui, T.; Berthet, J.-C.; Thuéry, P.; Salmon, L.; Rivière, E.; Ephritikhine, M. Lanthanide(III)/Actinide(III) Differentiation in the Cerium and Uranium Complexes [M($C_5Me_5$)$_2$(L)]0,+ (L=2,2′-Bipyridine, 2,2′:6′,2′′-Terpyridine): Structural, Magnetic, and Reactivity Studies. *Chem. Eur. J.* **2005**, *11*, 6994-7006.

[22] Sherbow, T. J.; Fettinger, J. C.; Berben, L. A. Control of Ligand pKa Values Tunes the Electrocatalytic Dihydrogen Evolution Mechanism in a Redox-Active Aluminum(III) Complex. *Inorg. Chem.* **2017**, *56*, 8651-8660.

[23] Knijnenburg, Q.; Smits, J. M. M.; Budzelaar, P. H. M. Reaction of the Diimine Pyridine Ligand with Aluminum Alkyls: An Unexpectedly Complex Reaction. *Organometallics* **2006**, *25*, 1036-1046.

[24] Sandoval, J. J.; Palma, P.; Álvarez, E.; Rodríguez-Delgado, A.; Cámpora, J. Dibenzyl and diallyl 2,6-bisiminopyridinezinc(ii) complexes: selective alkyl migration to the pyridine ring leads to remarkably stable dihydropyridinates. *Chem. Commun.* **2013**, *49*, 6791-6793.

[25] Sandoval, J. J.; Álvarez, E.; Palma, P.; Rodríguez-Delgado, A.; Cámpora, J. Neutral Bis(imino)-1,4-dihydropyridinate and Cationic Bis(imino)pyridine σ-Alkylzinc(II) Complexes as Hydride Exchange Systems: Classic Organometallic Chemistry Meets Ligand-Centered, Biomimetic Reactivity. *Organometallics* **2018**, *37*, 1734-1744.

[26] Sandoval, J. J.; Palma, P.; Álvarez, E.; Cámpora, J.; Rodríguez-Delgado, A. Mechanism of Alkyl Migration in Diorganomagnesium 2,6-Bis(imino)pyridine Complexes: Formation of Grignard-Type Complexes with Square-Planar Mg(II) Centers. *Organometallics* **2016**, *35*, 3197-3204.

[27] Zhang, G.; Wu, J.; Zeng, H.; Neary, M. C.; Devany, M.; Zheng, S.; Dub, P. A. Dearomatization and Functionalization of Terpyridine Ligands Leading to Unprecedented Zwitterionic Meisenheimer Aluminum Complexes and Their Use in Catalytic Hydroboration. *ACS Catal.* **2019**, *9*, 874-884.

[28] Gallardo-Villagrán, M.; Vidal, F.; Palma, P.; Álvarez, E.; Chen, E. Y. X.; Cámpora, J.; Rodríguez-Delgado, A. Aluminium(iii) dialkyl 2,6-bisimino-4R-dihydropyridinates(−1): selective synthesis, structure and controlled dimerization. *Dalton Trans.* **2019**, *48*, 9104-9116.

[29] Thompson, E. J.; Myers, T. W.; Berben, L. A. Synthesis of Square-Planar Aluminum(III) Complexes. *Angew. Chem. Int. Ed.* **2014**, *53*, 14132-14134.

[30]Capiomont, A.; Lajzerowicz-Bonneteau, J. Etude du radical nitroxyde tetramethyl-2,2,6,6 piperidine-1 oxyle-1 ou `tanane'. II. Affinement de la structure cristallographique de la forme quadratique desordonee. *Acta Crystallographica Section B* **1974**, *30*, 2160-2166.

[31] Sherbow, T. J.; Carr, C. R.; Saisu, T.; Fettinger, J. C.; Berben, L. A. Insight into Varied Reaction Pathways for O–H and N–H Bond Activation by Bis(imino)pyridine Complexes of Al(III). *Organometallics* **2016**, *35*, 9-14.

[32] Arnold, A.; Sherbow, T. J.; Sayler, R. I.; Britt, R. D.; Thompson, E. J.; Muñoz, M. T.; Fettinger, J. C.; Berben, L. A. Organic Electron Delocalization Modulated by Ligand Charge States in [L2M]n– Complexes of Group 13 Ions. *J. Am. Chem. Soc.* **2019**, *141*, 15792-15803.

[33] Langeslay, R. R.; Walensky, J. R.; Ziller, J. W.; Evans, W. J. Reactivity of Organothorium Complexes with TEMPO. *Inorg. Chem.* **2014**, *53*, 8455-8463.

[34] Smith, J. M.; Mayberry, D. E.; Margarit, C. G.; Sutter, J.; Wang, H.; Meyer, K.; Bontchev, R. P. N–O Bond Homolysis of an Iron(II) TEMPO Complex Yields an Iron(III) Oxo Intermediate. *J. Am. Chem. Soc.* **2012**, *134*, 6516-6519.

[35] Myers, T. W.; Berben, L. A. Aluminum–Ligand Cooperative N–H Bond Activation and an Example of Dehydrogenative Coupling. *J. Am. Chem. Soc.* **2013**, *135*, 9988-9990.

[36] Yang, L.; Powell, D. R.; Houser, R. P. Structural variation in copper(i) complexes with pyridylmethylamide ligands: structural analysis with a new four-coordinate geometry index, τ4. *Dalton Trans.* **2007**, 955-964.